EXPERIMENTAL ANALYSIS OF GAPS AND OVERLAPS CAUSED BY INTRA-PLY SECTORIZATION IN THE THERMOPLASTIC AUTOMATED FIBER PLACEMENT PROCESS

Thomas Zenker[1], Christian Schuerger[1] and Klaus Drechsler[2]

[1]Fraunhofer Institute for Chemical Technology ICT, Augsburg branch Functional Lightweight Design FIL, Am Technologiezentrum 2, 86159 Augsburg, Germany
Email: thomas.zenker@ict.fraunhofer.de, web page: http://www.ict.fraunhofer.de/en/comp/fil.html

[2]Institute for Carbon Composites, Technische Universitaet Muenchen
Boltzmannstr. 15, 85748 Garching, Germany

Keywords: Automated Fiber Placement, thermoplastic, defects, gaps, experimental

Abstract
Characteristic gaps and overlaps were analyzed experimentally for sectorized preforms of unidirectional tape with thermoplastic matrix. Laminates with different boundary configurations, layup sequences and staggering patterns were manufactured by the laser-assisted Automated Fiber Placement process. Thermographic analysis is carried out to determine the influence of generated local asperities on the layup process of subsequent plies. Preform homogeneity was analyzed manually and optically using a 3D-scanning device. Specimens were then consolidated using a hydraulic thermal press. Resulting fiber angle distribution in boundary areas was analyzed using an optical measurement technique. Correlation between perform surface homogeneity and in-plane undulation area size is shown.

1. Introduction

Automated Fiber Placement (AFP) is one of the most promising manufacturing technologies for the highly automated production of complex parts made of carbon fiber reinforced plastics (CFRPs). One main research points of the past years in the field of thermoplastic fiber placement was the optimization of the layup process for in-situ consolidation. This offers the possibility of producing parts from unidirectional tapes (UD-Tapes) in one single process step. Analysis has been conducted to find correlations between process parameters and the mechanical behavior of carbon fiber reinforced PEEK laminates on coupon level [1-3]. Hereto, different models have been proposed for the prediction of the degree of bonding achieved in the layup process. Grouve et at. [4] suggest a bonding model that is split in two simultaneously occurring phenomena, development of intimate contact of the laid tape with the substrate and polymer chain interdiffusion (healing). The model shows that for the material used, intimate contact development requires a longer time and is the main process velocity determining factor. A recent study [5] focusses on the bonding of PEEK-CF at nip point temperatures below the melting point. It is shown that bonding can occur below T_m if the polymer has first reached an amorphous state. This can allow faster processing speeds and rigid rollers with large laser shadows. Different prediction models [6-8] for the degree of bonding were analyzed for threshold temperatures of T_g and T_m and compared to experimental lap-shear results.

In-situ consolidation, so far, only proved to be achievable for flat geometries of full plies and where the process is used for simple winding. This is attributed to the complex control of process temperature and compaction pressure, related to the layup on a three dimensional tooling. When the process is used as a preforming technique however, the degrees of freedom of the robot based layup system offer unique

Excerpt from ISBN 978-3-00-053387-7

possibilities in terms of laminate design and fiber architecture. As an example, fibers can be laid down in curved paths in plane and in three dimensional shape (steering). Additionally, the implementation of adapted preform design - involving the use of tailored/ variable stiffness panels, drape-optimized 2.5D geometries, or load-path optimized, curved fibers - can be realized. By defining different layup zones with associated neutral fiber guide curves in geometrically complex parts, different fiber orientations can be achieved within one ply. This so-called intra-ply sectorization often involves a change of fiber direction on the sector boundary, which results in the formation of characteristic triangular gaps or overlaps in tow drop off areas.

Literature reports the effects of defects on laminate quality and mechanical behavior of thermoset based CFRPs. The effects of microbuckling were studied early analytically and experimentally for compression [9-11] and flexural strength [12]. Theoretical modelling of the influence of AFP induced defects in variable stiffness panels was conducted [13–15]. Falco et al. [16] further experimentally studied the influence of different manufacturing parameters, such as overlap coverage and ply staggering, by performing un-notched and open hole tensile tests. Lan et al. [17] studied the influence of a caul plate for autoclave polymerization on microstructure and tensile properties of different gap and overlap configurations. Croft et al. [18] investigated the influence of different characteristic AFP defect types (gap, overlap, half gap/overlap and twisted tow) on various mechanical properties on lamina and laminate level.

To the authors' knowledge, no experimental study on the effects of defects is available for thermoplastic AFP (TAFP) processing. It is hypothecated that the characteristic thermoplastic process parameters might lead to different results, in terms of defect size and fiber orientation, in contrast to the thermoset based process, especially when further processing of TAFP manufactured preforms is considered.

2. Experimental work

2.1 Material

Two pre-impregnated UD-tape materials with polyetheretherketone (PEEK) as matrix and S2-Glass Fiber (GF) and AS4-Carbon fiber (CF) reinforcement supplied by TenCate were used for the purpose of this study. The fiber volume fraction lies at 59 % ±3% for the PEEK-CF tape, and at 56 ± 3/-7 % in case of PEEK-GF. The 160 mm wide base tapes were cut into 6.35 mm tows using a tape slitter. As reported by [19], the possibility to heat up GF-reinforced material with diode laser systems is strongly limited due to the low absorption potential (a < ~10%) of the material in the wavelength spectrum emitted by the laser. Therefore, GF-tape with soot-particle additive was selected in order to enlarge the absorption band.

2.1 Processing technology

Tapes were laid on a flat, heated aluminum tooling, which is mounted on the vertical positioner system of the work cell, using a Coriolis Composites robot based, seven axes AFP machine. The machine allows the simultaneous lay-up of eight 6.35 mm tows with feed and cut. For the processing of thermoplastic pre-preg material, a diode laser unit (wavelength λ = 950 – 1040 nm) is used as a primary heat source. The used laser optic / homogenizer configuration creates a rectangular, homogenous laser field with dimensions of ~ 6.5 mm x 53.3 mm (in terms of an intensity drop of < 20 %). To ensure proper first ply adhesion, a polyimide film (Kapton HN 200, t = 50 µm) is applied to the surface using vacuum technique. (Figure 1) For temperature data online monitoring and recording, an FLIR A325sc infrared thermography camera, is attached to the laser optic mounting system. Preliminary tests were conducted to define the processing parameters for each of the CF- and GF tapes applied. Tests show that for equal feedrate and laser power, PEEK-GF showed a 7 -11% decrease in terms of average nip point temperature compared to PEEK-CF. Consequently, material specific velocity controlled heating profiles were defined for a constant temperature of 400 °C in order to ensure equivalent processing conditions for both materials.

Excerpt from ISBN 978-3-00-053387-7

For further analysis, sample preforms were consolidated into laminates in a thermal hydraulic press, equipped with a closed mold.

2.3 Specimen design and preparation

The setup design of the specimens under investigation in this study is schematically presented in Figure 2. The specimen is divided into two sectors, labeled S1 and S2, with associated guide curves (GC_S1, GC_S2), providing a fiber orientation of -5° and +5° to the neutral fiber direction (0°), respectively. The sector boundaries were defined rectangular with edges being parallel to GC_S1 and dimensions of 450 x 190 mm. The distance between GC_S1 and the edge shared by both sectors was defined to 25,4 mm, which equal half course width. This ensures that the outer tow edge of course 1 coincides with the sector boundary, which is necessary to have defined overlap shaping. This is taken as a basis for all prepared specimens.

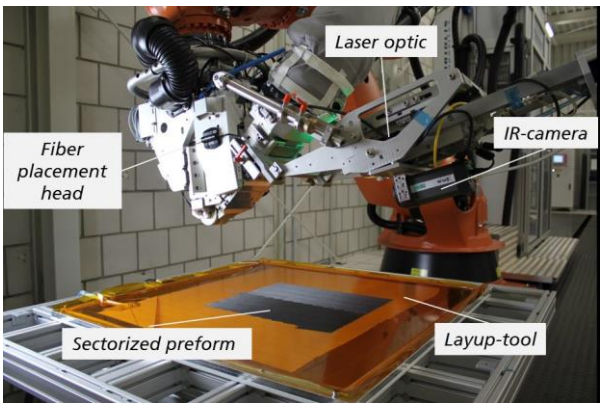

Figure 1. Fiber Placement machine setup

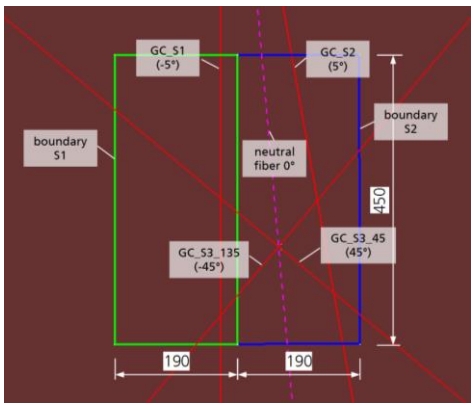

Figure 2. Schematic specimen design

The design of the sector boundary zone can be controlled by the overlap fraction (O) of S2. $O_{S2} = 0\%$ results in none of S2 tows crossing the sector boundary, leaving characteristic triangular gaps in the area of S2. $O_{S2} = 100\%$ means that the area of S2 is fully covered by S2 tows, resulting in triangular overlaps in the S1 area. Figure 3 visualizes the different boundary designs used in this study (gaps in red, overlaps in yellow).

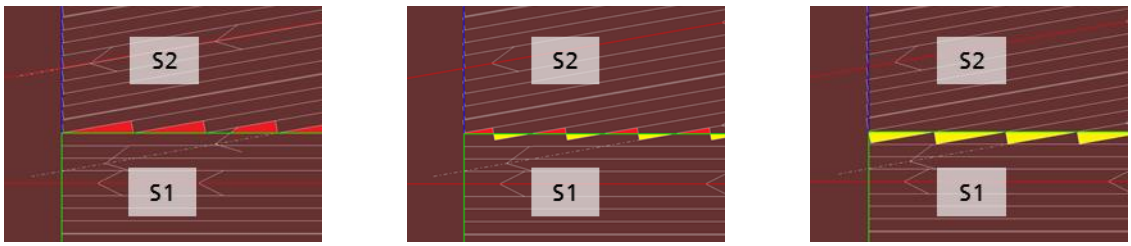

Figure 3. Boundary design by overlap parameter: $O_{S2} = 0\%$, $O_{S2} = 50\%$, $O_{S2} = 100\%$

Table 1 summarizes the configurations including O, staggering and material variations. All specimen of series 1 consist of eight plies. In configurations A-C, different boundary designs were investigated with specimen containing sectorized plies only. For configurations D-F, an additional sector, labeled S3, is defined as the sum of S1 and S2 to represent full plies. Corresponding guide curves are defined in such a way that fibers are oriented in ±45° to the neutral fiber direction.

To study the potential influence of defects on the application of subsequent plies containing the defect area, additional specimens are designed (X-Z, referred to as series 2). Here, specimens include one 0°

Excerpt from ISBN 978-3-00-053387-7

full first ply working as a substrate, ply_2 contains the defect with variable O, and ply_3 a 0° tape with the guide curve coinciding with the sector boundary.

Table 1. Overview specimen design

Series 1: Test setup for laminate characterization				
Configuration	Stacking	O	Staggering	Material
A	(0,10)8	0%/100%	no	GF
B	(0,10)8	0%/100%	yes	GF
C	(0,10)8	50%	yes	GF
C*	(0,10)8	50%	yes	CF
D	[(0,10)2/+45/-45]s	0%/100%	yes	GF
D*	[(0,10)2/+45/-45]s	0%/100%	yes	CF
E	[+45/-45/(0/10)2]s	0%/100%	yes	GF
F	[(0/10)2/+45/-45]s	0%	yes	GF
Series 2: Test setup for layup process optimization				
X	0/(0,10)/0	0%	no	CF
Y	0/(0,10)/0	50%	no	CF
Z	0/(0,10)/0	100%	no	CF

2.5 Preform characterization

To analyze the resulting preform quality, physical measurements were accompanied by optical analysis methods. A digital thickness dial gauge with a ball pin tip was used to measure the preform thickness deviations along the boundary zone. For each configuration, areas with highest (O_0) and lowest (G_0) thickness were determined in the sample region. These locations were then patterned in GC_S1 direction along the sector boundary (O_i, G_i). As reference, preform thickness in non-boundary areas was measured at points P_j in 100 mm distance to the outer preform boundaries. The local defect size o_i / g_i was then defined as the fraction of local extremum and average preform thickness.

Optical analysis was performed using an ATOS Core300 3D scanning device by GOM, Braunschweig, Germany, to measure gap and overlap sizes. To avoid misleading measurements due to preform warpage upon demolding, specimens were fixed onto a scanning table, using adequate clamping fixtures. Gap and overlap peaks were labeled in consistency to the nomenclature used for physical measurements. To compensate global warpage, additional reference points (Q_{ik} / F_{ik}) in 20 mm distance perpendicular to GC_S1 were defined. Eq.1 shows the corresponding defect size calculation.

$$o_i = \frac{O_i}{\frac{Q_{i1} + Q_{i2}}{2}} \tag{1}$$

Figure 4 visualizes an exemplary measurement grid for configuration B.

Excerpt from ISBN 978-3-00-053387-7

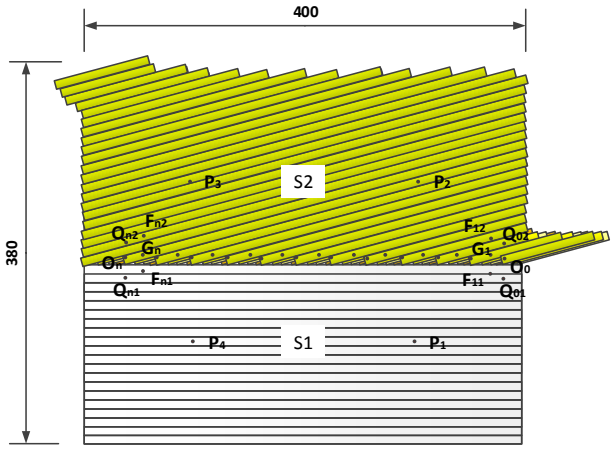

Figure 4. Thickness measurement grid configuration B

A dimensionless parameter h is defined to characterize the homogeneity of the surface (Eq.2).

$$h = 1 - \frac{\sum_{i=1}^{n}(o_i - g_i)}{n * t_{Preform}} \tag{2}$$

Finally, to analyze the influence of the various processing temperatures on pre-consolidation during the lay-up process, wedge peel tests were performed. Five specimens were tested for each configuration.

2.4 Laminate characterization

After preform consolidation, the ATOS Core300 optical measurement system was used to analyze surface topology. For the analysis of in plane undulations, Apodius Vision System (AVS) was used. Measured sector orientations α / β are defined as the local maxima of the fiber orientation distribution frequency $n(\varphi)$ within the analyzed area of 130 × 130 mm at the specimen center. In order to compare the amount of undulation occurrence between the various preforms under investigation, a fiber distribution frequency was integrated over the tolerance range of the angle. Maximum tolerable angular deviation was defined to 3°, leading to the integral form presented in Eq.3.

$$u = \int_{\alpha-3°}^{\alpha+3°} n(\varphi)d\varphi + \int_{\beta-3°}^{\beta+3°} n(\varphi)d\varphi \tag{3}$$

3. Results and discussion

3.1 Preform surface homogeneity

Figure 5 shows an exemplary section of the 3D topology scan of configurations E and F.

Excerpt from ISBN 978-3-00-053387-7

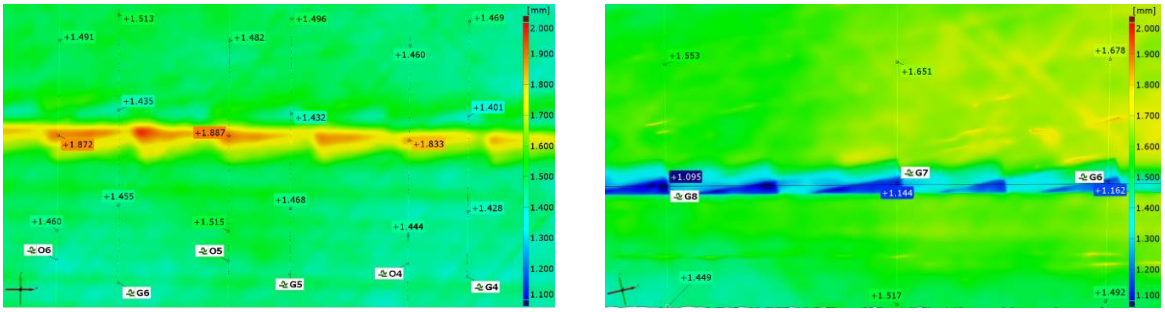

Figure 5. Example ATOS measurement results (Configuration E, F)

Figure 6 summarizes the preform thickness results measured using both dial gauge and the ATOS optical system.

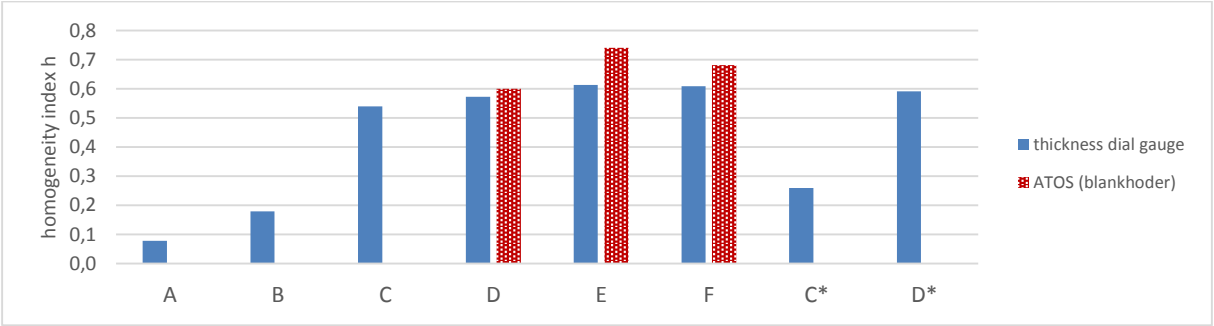

Figure 6. Preform homogeneity index h for different specimen configurations

A comparison between configurations A and B shows that the application of a staggering rule has positive influence on preform homogeneity. C shows a significantly more homogenous surface in contrast to A and B. Further the addition of full plies (D-E) leads to a far more homogenous surface. Comparing D and E, it can be observed that the stacking order does not have significant influence on homogeneity. Both configurations yield a homogeneity increase of > 200% compared to B, while defect ply fracture only decreased by 50%. Among the GF preforms, configurations E and F show the most homogenous surface.

It is to be noted that specimen C* is composed of only has half the number of plies compared to reference C. Assuming direct proportionality between defect layer amount and homogeneity, h(C*) can be doubled for direct comparison to h(C). Then, the deviation here as well as between D and D* is below 4%. This leads to the conclusion that the fiber types under consideration does not have significant influence on the homogeneity of a specific defect configuration.

3.2 Influence on layup process

Figure 7 shows the temperature profiles of series 2 specimen's ply 3, Figure 7 the corresponding average temperature values and average temperature standard deviations of each picture.

Excerpt from ISBN 978-3-00-053387-7

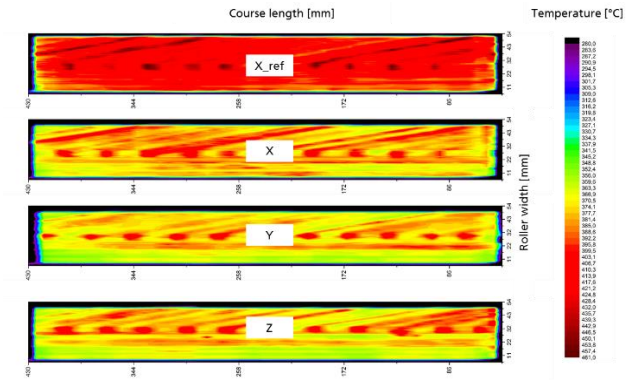

Figure 7. Temperature profiles series 2 (ply 3)

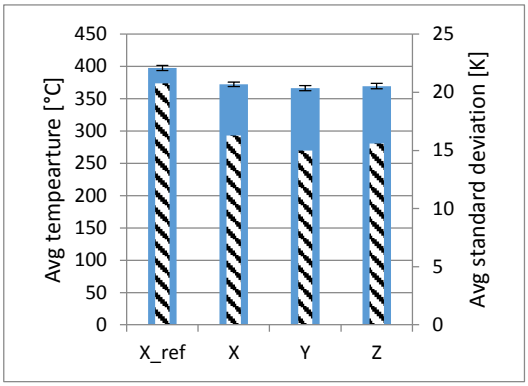

Figure 8. Average temperature and standard deviations [K]

For X_ref, it can be observed, that at the overlap points in P2 the maximum temperature exceeds the permissible working range. Thus, surface inhomogeneity seems to have a direct effect on the amount of absorbed energy input. The peak areas inside S2 are due to the previously observed correlation of substrate orientation and energy absorption potential. These can be compensated by defining substrate specific heating profiles when full plies with constant orientation is applied. This remains, however, only possible when the lay-up roller does not cross the sector line. As a near solution, laser power was reduced by 10% (X-Z). The resulting temperature profiles lie within the suggested temperature range of processing, given by the material supplier. A temperature drop of ~25 K from X_ref to X can be observed. Figure 11 shows the corresponding wedge peel test results.

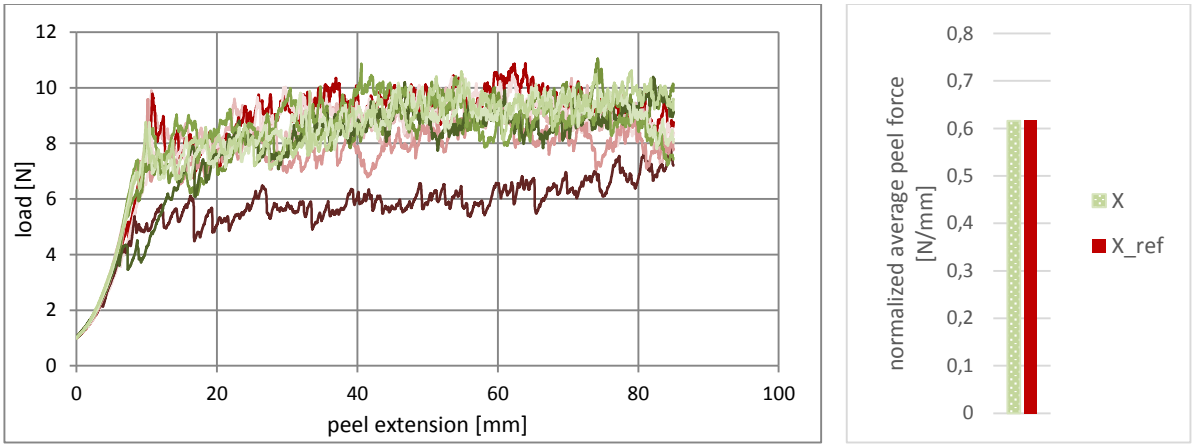

Figure 9. Results wedge peel test, load [N] over peel extension [mm], normalized average peel force [N/mm]

Wedge peel results indicate no significant reduction of peel strength due to reduced lay-up temperature. Peel force (average values from 10 mm to 85 mm peel extension) only drop by 1% on an average of 5 specimens. When comparing the different configurations in terms of heating homogeneity, it can be said that Y shows the most homogenous temperature distribution and lowest absolute average temperature. However, differences between configurations are rather small, no configuration exceeds the temperature processing window.

3.3 Laminate surface homogeneity and out of plane undulation

ATOS measurements of laminate configuration A yield a homogeneity index of 0,993. This means, even the most inhomogeneous preform of the considered specimen leads to a very plane surface after press consolidation. Microsections of the defect area zones show good consolidation for all laminates without any major porosity.

Excerpt from ISBN 978-3-00-053387-7

3.4 Laminate in-plane fiber undulation

Figure 10 shows the fiber angle detection routine of the AVS. Image a is the raw data picture gathered by the system, b shows a screenshot of the automatic fiber angle analysis routine. Sectors and boundary zones can be clearly identified, in boundary-near S2-areas with undulations, various fiber angles are detected. Diagram c shows the corresponding histogram. Fiber orientations $\alpha = -2.3°$ and $\beta = -12.5°$ are measured, the resulting angular difference of 10.2 ° corresponds to the relative orientation of the sector definition.

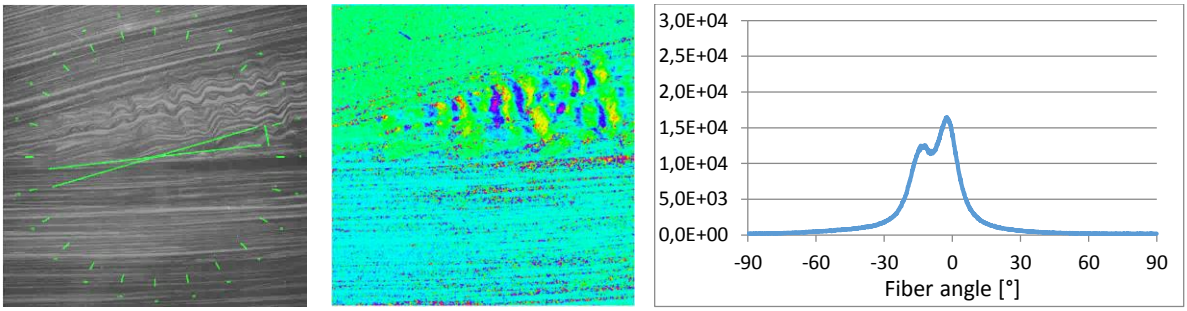

a b c

Figure 10. AVS fiber angle detection Configuration A

In comparison, Figure 9 shows the same images for configuration F, containing hardly any fiber undulation. Consequently, peaks in the histogram (image c) are sharper.

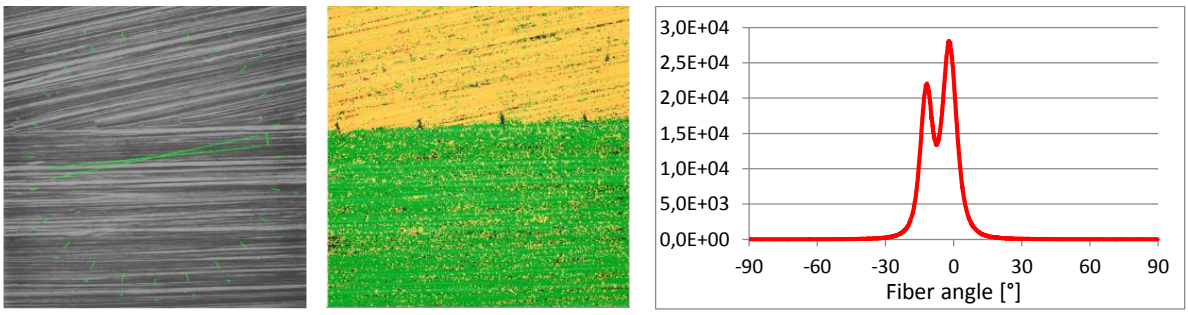

a b c

Figure 11. AVS fiber angle detection Configuration F

The fiber angle distributions of the other configurations and the results of the integration over the angular tolerance areas are displayed in Figure 12.

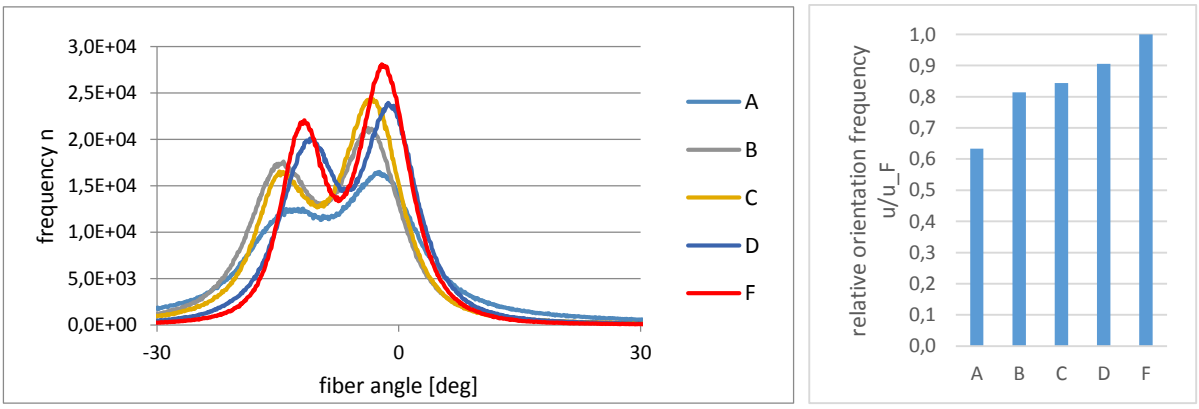

Figure 12. AVS fiber angle distributions and orientation frequency u in fraction of Configuration F

Excerpt from ISBN 978-3-00-053387-7

Correlation can be observed between undulation quantity and surface topology. Configurations A and B show most fiber orientation deviations. C shows a light improvement. Full plies seem to further reduce undulations (D, F). The difference between D and F is bigger than the homogeneity index indicates. This might be due to the absence of overlaps in F. Flow processes in closed mold press consolidation are assumed to be the main cause for fiber buckling. Overlaps can be seen as stress concentration areas during heating phase and might initiate compression bucking when temperature locally reaches T_m.

4. Conclusion and outlook

Different application oriented configurations of boundary zone designs were processed and experimentally investigated. Design parameters were found to have significant influence on preform surface homogeneity. Press consolidation compensates all asperities in terms of surface flatness. However in-plane undulations were found in boundary regions near S2. Fiber angle deviation measurements suggest a correlation between preform homogeneity and undulation extent. Generally, an overlap free configuration with additional full plies was found to have least fiber disorientations.

Further work has to be carried out to characterize the influence of different defect configurations on mechanical performance. A detailed analysis of the microsections in terms of possible local out of plane undulation in respect to laminate configuration can help to explain consolidation behavior. Moreover, a flow simulation of the consolidation process seems to be the key to technology transfer from coupon level to complex geometries.

Acknowledgments

The author would like to thank the Federal Ministry for Economic Affairs and Energy (BMWI) for funding this research within the GeKo-Therm project as part of the LuFo V call.

References

[1] C.M. Stokes-Griffin and P. Compston. The effect of processing temperature and placement rate on the short beam strength of carbon fibre–PEEK manufactured using a laser tape placement process. *Composites Part A: Applied Science and Manufacturing*, 78: 274–283, 2015.
[2] A.J. Comer, D. Ray, W.O. Obande, et al. Mechanical characterisation of carbon fibre–PEEK manufactured by laser-assisted automated-tape-placement and autoclave. *Composites Part A: Applied Science and Manufacturing*, 69: 10–20, 2015.
[3] Z. Qureshi, T. Swait, R. Scaife and H.M. El-Dessouky. In situ consolidation of thermoplastic prepreg tape using automated tape placement technology: Potential and possibilities. *Composites Part B: Engineering*, 66: 255–267, 2014.
[4] W.J.B. Grouve, L.L. Warnet, B. Rietman, H.A. Visser and R. Akkerman. Optimization of the tape placement process parameters for carbon–PPS composites. *Composites Part A: Applied Science and Manufacturing*, 50: 44–53, 2013.
[5] C.M. Stokes-Griffin and P. Compston. Investigation of sub-melt temperature bonding of carbon-fibre/PEEK in an automated laser tape placement process. *Composites Part A: Applied Science and Manufacturing*, 84: 17–25, 2016.
[6] M.A. Khan, P. Mitschang and R. Schledjewski. Parametric study on processing parameters and resulting part quality through thermoplastic tape placement process. *Journal of Composite Materials*, 47: 485–499, 2013.
[7] J. Tierney. Modeling of In Situ Strength Development for the Thermoplastic Composite Tow Placement Process. *Journal of Composite Materials*, 40: 1487–1506, 2006.
[8] S.C. Mantell and G.S. Springer. Manufacturing Process Models for Thermoplastic Composites. *Journal of Composite Materials*, 26: 2348–2377, 1992.
[9] E.G. Guynn, W.L. Bradley and O.O. Ochoa. A Parametric Study of Variables That Affect Fiber Microbuckling Initiation in Composite Laminates: Part 2 -- Experiments. *Journal of Composite Materials*, 26: 1617–1643, 1992.

[10] P. Berbinau, C. Soutis and I.A. Guz. Compressive failure of 0° unidirectional carbon-fibre-reinforced plastic (CFRP) laminates by firebre microbuckling. *Composites Science and Technology*: 1451–1455, 1999.
[11] H.M. Hsiao and I.M. Daniel. Effect of fiber waviness on stiffness and strength reduction of unidirectional composites under compressive loading. *Composites Science and Technology*, 56: 581–593, 1996.
[12] R. Marissen and H.R. Brouwer. The signifcance of fibre microbuckling for the flexural strength of a composite. *Composites Science and Technology*: 327–330, 1999.
[13] A.W. Blom, C.S. Lopes, P.J. Kromwijk, Z. Gurdal and P.P. Camanho. A Theoretical Model to Study the Influence of Tow-drop Areas on the Stiffness and Strength of Variable-stiffness Laminates. *Journal of Composite Materials*, 43: 403–425, 2009.
[14] K. Fayazbakhsh, M. Arian Nik, D. Pasini and L. Lessard. Defect layer method to capture effect of gaps and overlaps in variable stiffness laminates made by Automated Fiber Placement. *Composite Structures*, 97: 245–251, 2013.
[15] X. Li, S.R. Hallett and M.R. Wisnom. Modelling the effect of gaps and overlaps in automated fibre placement (AFP)-manufactured laminates. *Science and Engineering of Composite Materials*, 22, 2015.
[16] O. Falcó, J.A. Mayugo, C.S. Lopes, N. Gascons and J. Costa. Variable-stiffness composite panels: Defect tolerance under in-plane tensile loading. *Composites Part A: Applied Science and Manufacturing*, 63: 21–31, 2014.
[17] M. Lan, D. Cartié, P. Davies and C. Baley. Microstructure and tensile properties of carbon–epoxy laminates produced by automated fibre placement: Influence of a caul plate on the effects of gap and overlap embedded defects. *Composites Part A: Applied Science and Manufacturing*, 78: 124–134, 2015.
[18] K. Croft, L. Lessard, D. Pasini, M. Hojjati, J. Chen and A. Yousefpour. Experimental study of the effect of automated fiber placement induced defects on performance of composite laminates. *Composites Part A: Applied Science and Manufacturing*, 42: 484–491, 2011.
[19] Brecher C, Emonts M, Schares RL and Stimpfl J (eds). *CO2-laser-assisted processing of glass fiber-reinforced thermoplastic composites*: SPIE, 2013.

Excerpt from ISBN 978-3-00-053387-7